Effects of Thickness Extension Mode Resonance Oscillation of Acoustic Waves on Catalytic and Surface Properties. 5. Effects of Ferroelectric Crystal Thickness on the Catalytic Behavior of Ag for Ethanol Decomposition

Y. Yukawa, N. Saito, H. Nishiyama, and Y. Inoue*

Department of Chemistry, Nagaoka University of Technology, Nagaoka 940-2188, Japan

Received: January 9, 2004; In Final Form: May 29, 2004

The five kinds of ferroelectric z-cut $LiNbO_3$ crystals with different thicknesses of 0.3, 0.5, 1.0, 2.0, and 2.2 mm were employed to reveal the effects of frequency in thickness extension mode resonance oscillation (TERO) of acoustic waves on the catalytic properties of a 100 nm thick Ag film deposited onto the crystals. The different thicknesses of the crystals provided 11.2, 7.3, 3.6, 1.8, and 1.6 MHz as the primary resonance frequency, respectively. In ethanol decomposition producing ethylene and acetaldehyde, the characteristics of the TERO that caused significant increases in catalytic activity for ethylene production were observed for the five frequencies, but the extent of activity increments depended on the frequency: a maximum appeared at a medium frequency of 7.3 MHz. Remarkably large decreases in the activation energy for ethylene production occurred with 1.6−1.8 MHz, compared to those of the rest of the frequencies. Laser Doppler measurements showed the different distributions of lattice displacement among the five frequencies. The frequency dependence of catalytic activity enhancement was associated with both the magnitudes of lattice displacement and the density of sites causing lattice displacement. Markedly large distortion due to lattice displacement was observed for 1.6−1.8 MHz, compared to the high frequencies, and is considered to be responsible for large activation energy decreases with the lower frequency. The frequency effects of different crystal thicknesses on catalytic behavior are discussed.

Introduction

We have so far studied the effects of acoustic waves on the activity and reaction selectivity for the various kinds of reactions on thin metal catalysts deposited on the ferroelectric materials.[1−17] Among the different vibration modes of acoustic waves, thickness extension mode resonance oscillation (TERO) generated on a ferroelectric z-cut $LiNbO_3$ crystal increased the selectivity for ethylene production remarkably with a small influence on acetaldehyde production in the ethanol decomposition over Ag and Pd catalysts deposited on the crystal. For a better understanding of a mechanism of TERO-induced catalyst activation, it is of particular importance to elucidate the effects of resonance frequency on catalytic activity and reaction selectivity. Two methods are available for generation of the different resonance frequencies. One is the employment of an overtone resonance frequency that appears as a series of resonance frequencies such as the first, the second, the third, and so on. Recently, the TERO effects of overtone resonance frequencies (10.8 and 17.9 MHz) in addition to a primary resonance frequency (3.5 MHz) have been examined for ethanol decomposition on a Ag catalyst.[17] The efficiency of catalyst activation strongly depended on the resonance frequency. In a low radio frequency (rf) power region, the catalyst activation for ethylene production had a maximum at a medium frequency of 10.8 MHz, whereas in a high power region, it became larger in the order 3.5 MHz > 10.8 MHz > 17.9 MHz.

The other method is the employment of the ferroelectric crystal with different crystal thicknesses, since resonance frequency is inversely proportional to crystal thickness in the TERO mode with spontaneous polarization vertical to the surface.[18] A clear difference between an overtone frequency and a thickness-induced frequency is that the former is generated for the same thickness of a ferroelectric crystal, whereas the latter is generated under the crystal conditions of different thicknesses. Thus, there is a possibility that the extent of crystal distortion due to TERO is different between them. Furthermore, it is interesting to see how the TERO effects vary with the thickness of a ferroelectric crystal, since no such study has been performed. In the present study, five z-cut $LiNbO_3$ crystals with various thicknesses were employed for ethanol decomposition on a Ag catalyst, and it has been revealed that the TERO effects on the catalysis are intrinsically different in a lower frequency regime.

Experimental Section

Five ferroelectric z-cut $LiNbO_3$ (z-LN) single crystals with thicknesses of 0.3, 0.5, 1.0, 2.0, and 2.2 mm were used as substrates. The crystals were cut into a square of 14 mm × 14 mm. The catalyst was prepared by depositing a Ag metal film at a thickness of 100 nm on the front and back planes of the crystals by resistance heating of a 99.99% pure Ag block in a vacuum.

Rf electric power was imposed to a catalyst by the same method using a network analyzer, an amplifier, and a network tuner, which was described elsewhere.[15] A closed gas-circulating reaction apparatus equipped with a gas chromatograph for product analysis was used, and the catalytic reaction of ethanol decomposition was carried out at an ethanol pressure of 4.0 kPa and in the temperature range 593−623 K. Care was taken to maintain a constant catalyst temperature with the rf power

* Corresponding author.

10.1021/jp049891d CCC: $27.50
Published on Web 12/04/2004

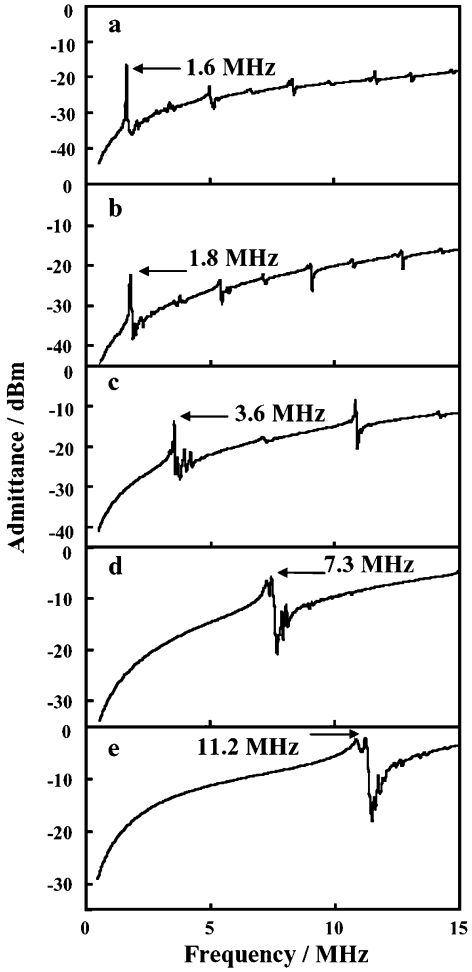

Figure 1. Resonance lines of z-LN with crystal thicknesses of 2.2 (a), 2.0 (b), 1.0 (c), 0.5 (d), and 0.3 (e) mm.

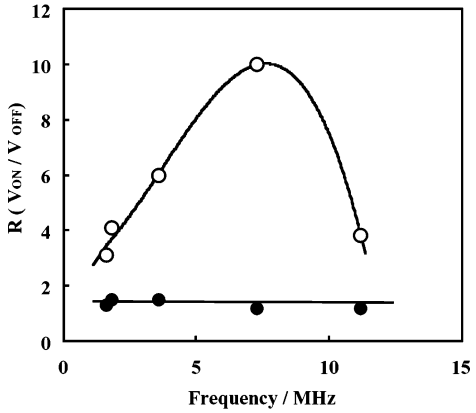

Figure 2. Activation coefficients for ethylene, R_e (○), and acetaldehyde, R_a (●), as a function of frequency. Rf power $J = 1$ W, and reaction temperature $T_R = 613$ K.

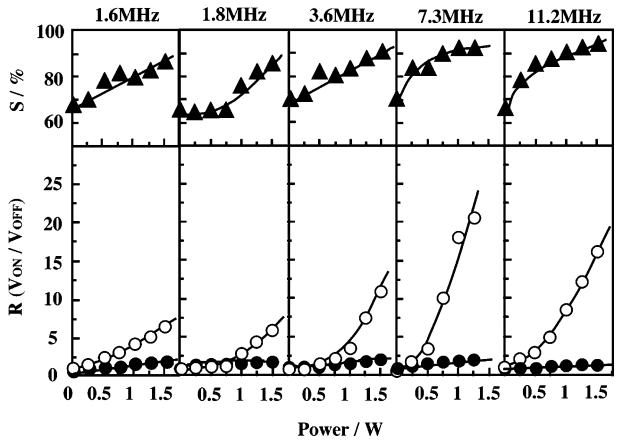

Figure 3. Changes in activation coefficients for ethylene, R_e (○), and acetaldehyde, R_a (●), and in selectivity for ethylene production, S (▲), with increasing rf power.

off and on. The temperature of the catalyst was monitored from resonance frequency by taking advantage of the high sensitivity of the frequency to temperature and controlled by an outer electric furnace within ±1 K.

Three-dimensional laser Doppler images were obtained to monitor the magnitudes and density of lattice displacement. The method and apparatus were described elsewhere.[6]

Results

Figure 1 shows the characteristic resonance lines of the five crystals. The first resonance frequency appeared at 1.6, 1.8, 3.6, 7.3, and 11.2 MHz for the thicknesses of $t = 2.2$, 2.0, 1.0, 0.5, and 0.3 mm, respectively. The frequency increased in inverse proportion to the thickness of the substrate ferroelectric crystals.

In all the catalytic runs on the five catalysts, the major products were ethylene and acetaldehyde, which were formed at constant reaction rates from the initial stages. In all the frequencies, TERO on caused immediate and dramatic increases in the activity for ethylene production but a small enhancement of the activity for acetaldehyde production. The enhanced activities for ethylene production were maintained while TERO was on and decreased to the original low levels with the TERO off. The activation coefficient, R, was defined as the ratio of activity with TERO on to that with TERO off (the subscripts e and a were attached to R to distinguish the activation coefficients for ethylene and acetaldehyde production, respectively).

Figure 2 shows changes in R_e and R_a for the five frequencies. Although the results for 3.6 MHz have already been reported in a previous study,[17] they are shown here again for the comparison of frequency effects, since it is beneficial to show them as a kind of standard rather than to intentionally exclude. R_e was 3.1 for 1.6 MHz, 4.1 for 1.8 MHz, 6.0 for 3.6 MHz, 10.0 for 7.3 MHz, and 3.8 for 11.2 MHz. R_e became larger with increasing frequency, reached a maximum at 7.3 MHz, and decreased considerably. On the other hand, R_a was 1.4 for 1.6 MHz, 1.6 for both 1.8 and 3.6 MHz, and 1.3 for both 7.3 and 11.2 MHz. Neither marked activity enhancement nor a clear maximum in the activity order for acetaldehyde production was observed.

Figure 3 shows R_e and R_a for the different frequencies as a function of rf power. For 1.6 MHz, R_e increased gradually with increasing power. For 1.8 MHz, a gradual enhancement of R_e was followed by a steep rise at around 1 W. For 3.6 MHz, a steep rise occurred at around 0.75 W. As the frequency became larger, there was a trend of the threshold rf power to bring about a steep rise of R_e at a lower power. Figure 3 also shows the selectivity for ethylene production, S, for the five frequencies as a function of rf power. With increasing frequencies, the large enhancement of S was induced at a low power.

Figure 4 shows the temperature dependence of the reaction in the temperature range 593−623 K. The activation energy for ethylene production with TERO off was calculated to be 140 kJ mol^{-1}. TERO on at 1 W for 1.6 MHz led to a smaller temperature dependence, which decreased the activation energy to 86 kJ/mol^{-1}. Table 1 shows activation energy as a function of TERO frequency. It should be noted that the activation energy

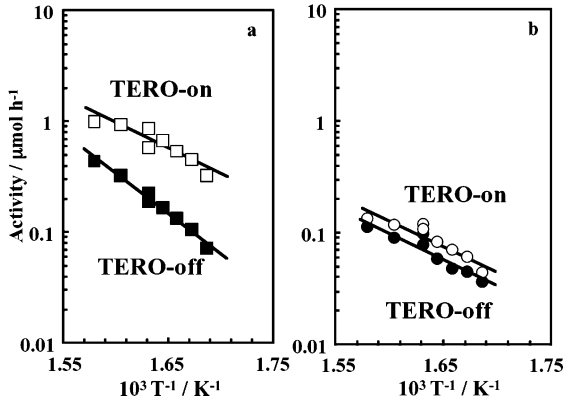

Figure 4. Temperature dependence of ethylene (a) and acetaldehyde (b) production with TERO off (■, ●) and TERO on (□, ○). Frequency $f = 1.6$ MHz, and $J = 1$ W.

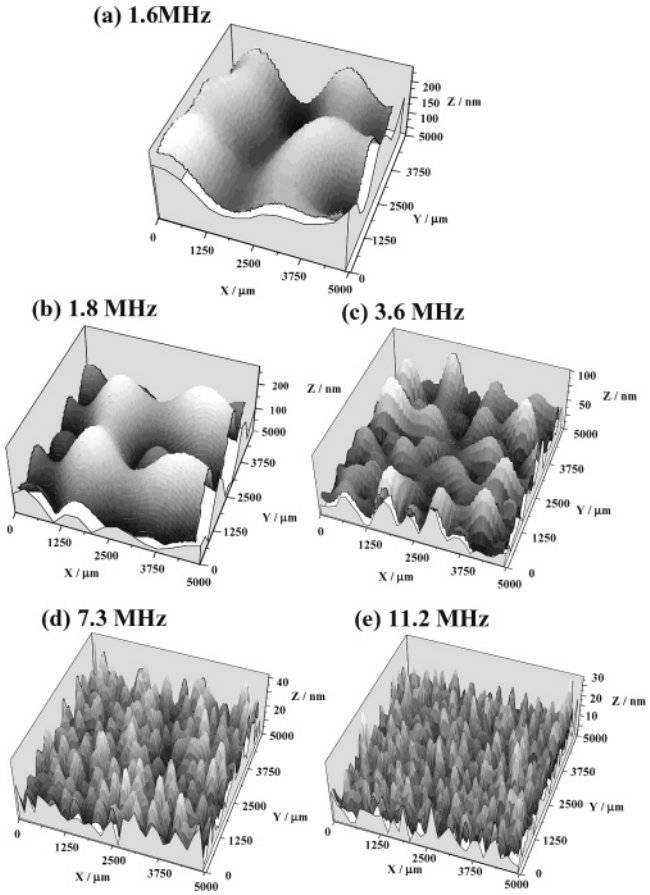

Figure 5. Three-dimension lattice displacement patterns with TERO on at 1.6 (a), 1.8 (b), 3.6 (c), 7.3 (d), and 11.2 (e) MHz. $J = 1$ W.

drop was small for 11.2 and 7.3 MHz, considerable for 3.6 MHz, and markedly large for 1.8 and 1.6 MHz.

Figure 5 shows three-dimensional laser Doppler patterns for the five frequencies at an rf power of 1 W. The patterns show the peaks that represent the amplitudes of standing waves, that is, the magnitudes of lattice displacement. The random distributions of the peaks were observed over the $x-y$ direction. For 1.6 MHz, large and broad peaks appeared. As the resonance frequency increased, the peaks became finer and smaller, but the number increased markedly. Figure 6 shows the distributions of peaks for the different frequencies. For 1.6 and 1.8 MHz, the peaks were so large that the largest lattice displacements, L_{max}, were 270 and 310 nm, and the average lattice displacements, L_{av}, reached 137 and 104 nm, respectively. For 7.3 MHz,

TABLE 1: Activation Energy for Ethylene and Acetaldehyde Production as a Function of Resonance Frequency[a]

		TERO on				
	TERO off	1.6 MHz	1.8 MHz	3.6 MHz	7.3 MHz	11.2 MHz
$E_{(CH)}$/kJ mol^{-1}	140	86	92	120	129	130
$E_{(CHO)}$/kJ mol^{-1}	93	87	87	87	87	87

[a] $E_{(CH)}$ = activation energy for ethylene production. $E_{(CH)}$ = activation energy for acetaldehyde production.

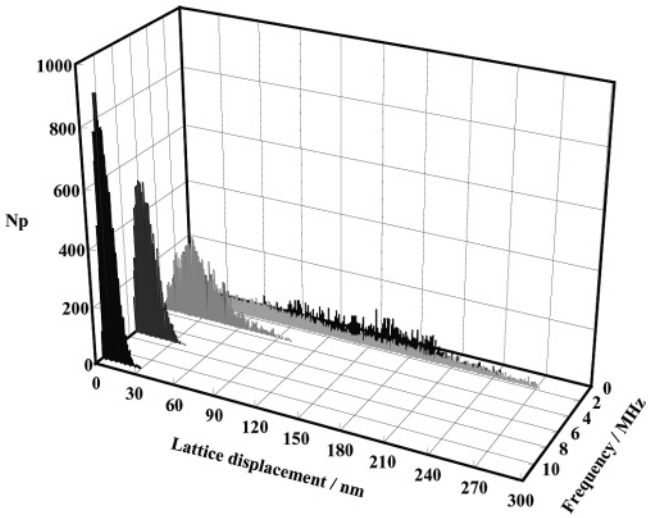

Figure 6. Distributions of lattice displacement with different frequencies.

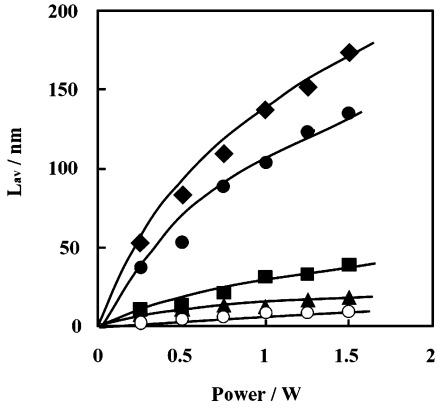

Figure 7. Average lattice displacement, L_{av}, at 1.6 (◆), 1.8 (●), 3.6 (■), 7.3 (▲), and 11.2 (○) MHz as a function of rf power.

the distribution became considerably narrower: L_{max} and L_{av} were 51 and 13 nm, respectively. For 11.2 MHz, the distribution was much narrower: L_{max} and L_{av} were 29 and 9 nm, respectively. Figure 7 shows changes in L_{av} for the five frequencies with rf power. L_{av} increased considerably in a low power regime, followed by gradual rises. The changes were represented by the correlation that L_{av} was in proportion to the square root of the rf power, which was consistent with a relationship derived from a piezoelectric equation.[19] The number of peaks per unit area, N_p, was counted, and Figure 8 shows changes in N_p and L_{av} with resonance frequency. The figure involves N_p and L_{av} obtained previously for the overtone frequency.[17] L_{av} decreased dramatically with increasing frequency from 1.6 to 1.8 to 3.6 MHz, followed by a gradual attenuation above 7.3 MHz. On the other hand, N_p was quite small for 1.6−1.8 MHz, and increased significantly from 3.6 to 17.9 MHz.

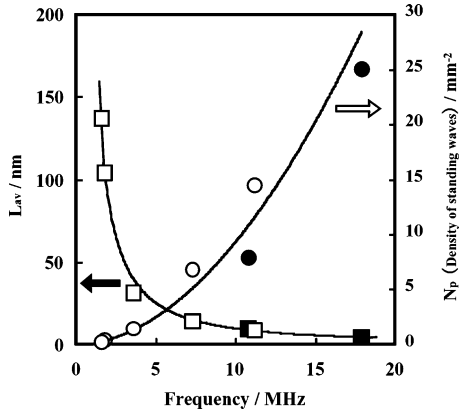

Figure 8. Changes in average lattice displacement, L_{av} (□), and density of standing waves, N_p (○), with frequency. Filled circles and squares are values for the overtone frequency (cf. ref 17).

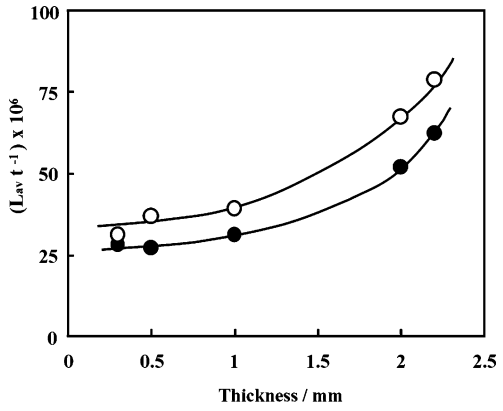

Figure 9. Ratio of average lattice displacement to crystal thickness, L_{av}/t, as a function of crystal thickness at rf powers of 0.5 W (●) and 1.0 W (○).

The ratio of L_{av} to crystal thickness, t, was evaluated for the different thicknesses of the ferroelectric crystals. Figure 9 shows changes in the L_{av}/t ratio with crystal thickness for two rf powers. The ratio increased slightly up to $t = 1$ mm and steeply with increasing thickness and reached markedly large levels at $t = 2.0$ mm (1.8 MHz) and $t = 2.2$ mm (1.6 MHz).

Discussion

Provided that resonance oscillation has a thickness extension mode, the frequency f_r is given by

$$f_r = \{(2n - 1)/2t\}(C_{33}^{E}/\rho)^{1/2}$$

where n is 1, 2, 3, or an integer, C_{33}^{E} is the elastic constant, t is thickness, and ρ is the density of a ferroelectric crystal.[18,19] The primary resonance frequency ($n = 1$) was calculated to be 1.7, 1.8, 3.7, 7.4, and 11.5 MHz for $t = 2.2$, 2.0, 1.0, 0.5, and 0.3 mm, respectively. The obtained values were consistent with the observed resonance lines of 1.6, 1.8, 3.6, 7.3, and 11.2 MHz, respectively. This confirms that the resonance oscillation of all these crystals has the vibration of thickness extension mode.

The general features of the TERO effects on selectivity enhancements and activation energy decreases for ethylene production were observed for the five frequencies. However, there was a distinct difference between 1.6 and 1.8 MHz and the other three frequencies. As shown in Table 1, activation energy decreases were markedly large for the former frequency group. This indicates that the effects of lattice displacement on the surface catalytic properties are significantly different between the two frequency groups.

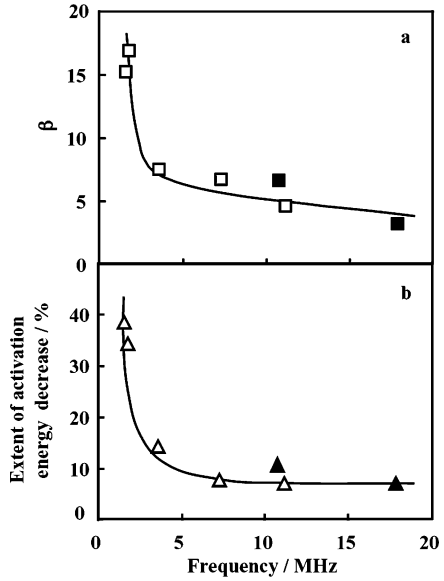

Figure 10. Changes in β (a) and the extent of activation energy decrease for ethylene production (b) with frequency. Filled squares and triangles are values for the overtone frequency (cf. ref 17).

In the laser Doppler images of TERO, the distributions of peaks due to standing waves widely varied with frequency, as shown in Figures 5 and 6. The low-frequency group of 1.6−1.8 MHz provided extremely broad distributions but small N_p. By contrast, the highest frequency exhibited a narrow distribution but an extraordinarily large N_p. In other words, the low-frequency group generated the large magnitudes of lattice displacement in small number, whereas the high-frequency group provided just the opposite relation. In a previous study using an overtone frequency,[17] it has been demonstrated that the catalytic activity enhancement by the TERO is associated with both L_{av} (L_{max}) and N_p. In the case that either L_{av} (L_{max}) or N_p is small, the activity enhancement remains to a small extent, and large activity increases are induced under the conditions where both are able to reach satisfactory levels. This view explains the appearance of a maximum in the frequency dependence of catalytic activity enhancement (Figure 2). However, as for amplitude effects, the extent of lattice displacement was intrinsically different with the thick ferroelectric crystals. As shown in Figure 9, the ratio of L_{av} to crystal thickness, L_{av}/t, was significantly large for $t = 2.0$ mm (1.8 MHz) and $t = 2.2$ mm (1.6 MHz), compared to those for the other crystals. This indicates that the thicker crystals have the ability to generate markedly large lattice displacement. By assuming that one standing wave is approximated to be a triangle shape such that the oblique side is y and the base is x, the ratio $y/x = \beta$ can be taken as a measure of distortion caused by lattice displacement. Figure 10a shows the plots of β vs frequency. The results for the overtone frequency obtained in a previous study[17] are added to the figure. The value of β was extraordinarily large at 1.6−1.8 MHz, dropped sharply at 3.6 MHz, and gradually decreased with increasing frequency up to 17.9 MHz. This demonstrates that the extent of distortion in TERO is markedly larger for 1.6−1.8 MHz than that for frequencies higher than 3.6 MHz.

As shown in Table 1, the activation energy for ethylene production decreased significantly with 1.6−1.8 MHz. It is of particular interest to see how the extent of activation energy drop is correlated with the parameter β. Figure 10b shows the

extent of activation energy decrease as a function of frequency. It was markedly large for 1.6−1.8 MHz, and a sharp attenuation occurred between 1.8 and 3.6 MHz, followed by a gradual decrease with increasing frequency. It should be noted that a change in the extent of activation energy drop with frequency is quite analogous to that in β. This indicates that the markedly large distortion caused by TERO is responsible for the large activation energy drop. Furthermore, these results suggest that there is a threshold in the distortion effect on catalytic properties, above which large changes in kinetic parameters are induced. Even though the geometric effects of TERO on the surface atom−atom distance and arrangement appear to be extremely small, there exists an effect on the extent to which the catalytic properties of the surface vary.

In a previous photoelectron emission spectroscopy (PES) study of Ag and Pd metals, we have demonstrated that the TERO (3.6 MHz) caused the positive shifts of the threshold energy for photoelectron emission.[13−16] The positive shifts are indicative of the enhancement of the work function. The work function shifts became larger with increasing lattice displacement of TERO, indicating that the vertical lattice displacement is responsible for work function increases. Furthermore, a recent study using photoelectron emission microscopy (PEEM) has demonstrated that the vertical lattice displacement of a surface acoustic wave caused a decrease in the PEEM intensity, i.e., a work function increase, of a low-index Cu surface such as Cu(111).[20] On the other hand, no work function changes have been reported for thickness-shear mode resonance oscillation (TSRO) that has a vibration mode parallel to the surface.[13,21] According to a jellium model,[22−24] the work function of transition metals is associated with an electric double layer formed at the topmost surface atoms by electrons that spill out toward a vacuum and by positive charges remaining inside a metal surface. Since the direction of electrons that spill out from the surface is consistent with the direction of lattice vibration, a mechanism with work function enhancement has been proposed on the basis of the assumption that the vertical lattice displacement increases the density of spill-out electrons.[13,14] As discussed in a previous paper,[13] the selectivity for ethylene production has been proposed to be associated with the different structures of ethanol adsorbed: the strongly adsorbed ethoxy species having an orientation with the C−C bond normal to the surface is responsible for acetaldehyde production, whereas the weakly chemisorbed ethanol with the O−H bond oriented parallel to the surface produces ethylene. The TERO effects on the promotion of ethylene production are explained in terms of the formation of the weakly chemisorbed ethanol by an increase in the work function.

To clarify the distortion effects on work function changes, it is desirable to obtain the photoemission spectra for a single standing wave. Unfortunately, in the photoelectron emission spectra so far obtained for 3.6 MHz, a light beam spot used for the measurements was too wide for the size of the waves, which provided average values resulting from a considerably large number of waves. The large standing waves generated at 1.6−1.8 MHz had nearly the same size as the beam spot. Since remarkably large lattice displacement occurred at 1.6−1.8 MHz, it would be expected that the low frequencies are able to cause large work function changes. This offers the advantage of measuring the characteristics of photoelectrons emitted from a single standing wave by employing a light beam as narrow as possible. A study is in progress.

Acknowledgment. This work was supported by a Grant-in-Aid of Scientific Research A (15206088) from The Ministry of Education, Science, Sports and Culture.

References and Notes

(1) Ohkawara, Y.; Saito, N.; Inoue, Y. *Surf. Sci*. **1996**, *357/358*, 777.
(2) Saito, N.; Ohkawara, Y.; Watanabe, Y.; Inoue, Y. *Appl. Surf. Sci.* **1997**, *121/122*, 343.
(3) Ohkawara, Y.; Saito, N.; Inoue, Y. *Chem. Phys. Lett.* **1998**, *286*, 502.
(4) Saito, N.; Ohkawara, Y.; Sato, K.; Inoue, Y. *MRS Symp. Proc.* **1998**, *497*, 215.
(5) Inoue, Y. *Catal. Surv. Jpn.* **1999**, *3*, 95.
(6) Saito, N.; Nishiyama, H.; Sato, K.; Inoue, Y. *Chem. Phys. Lett.* **1998**, *297*, 72.
(7) Saito, N.; Sato, K.; Inoue, Y. *Surf. Sci.* **1998**, *417*, 384.
(8) Saito, N.; Nishiyama, H.; Sato, K.; Inoue, Y. *Surf. Sci*. **2000**, *454/456*, 1099.
(9) Saito, N.; Sakamoto, M.; Nishiyama, H.; Inoue, Y. *Chem. Phys. Lett*. **2001**, *341*, 232.
(10) Ohkawara, Y.; Saito, N.; Inoue, Y. *Solid State Ionics* **2000**, *136/137*, 819.
(11) Saito, N.; Nishiyama, H.; Inoue, Y. *Appl. Surf. Sci*. **2001**, *169/170*, 259.
(12) Saito, N.; Inoue, Y. *J. Chem. Phys*. **2000**, *113*, 469.
(13) Saito, N.; Inoue, Y. *J. Phys. Chem. B* **2002**, *106*, 5011.
(14) Saito, N.; Yukawa, Y.; Inoue, Y. *J. Phys. Chem. B* **2002**, *106*, 10179.
(15) Yukawa, Y.; Saito, N.; Nishiyama, H.; Inoue, Y. *Surf. Sci.* **2002**, *502/503*, 527.
(16) Yukawa, Y.; Saito, N.; Nishiyama, H.; Inoue, Y. *J. Phys. Chem. B* **2002**, *106*, 10174.
(17) Saito, N.; Inoue, Y. *J. Phys. Chem. B* **2003**, *107*, 2040.
(18) Ikeda, T. *Fundamental of Piezoelectricity*; Oxford University Press: New York, 1990; p 117.
(19) Auld, B. A. *Acoustic Fields and Waves in Solids*; Wiley: New York, 1973; Vol. 2.
(20) Nishiyama, H.; Inoue, Y. *J. Phys. Chem. B* **2003**, *107*, 8738.
(21) Yukawa, Y.; Saito, N.; Nishiyama, H.; Inoue, Y. *Surf. Sci.* **2003**, *532/535*, 359.
(22) Lang, N. D.; Kohn, W. *Phys. Rev.* **1970**, *B1*, 4555.
(23) Smith J. R. *Phys. Rev*. **1969**, *181*, 522.
(24) Skriver, H. L.; Rosengaard, N. M. *Phys. Rev. B* **1992**, *46*, 7157.